Layer-by-Layer Assembled Mixed Spherical and Planar Gold Nanoparticles: Control of Interparticle Interactions

ARTICLE *in* LANGMUIR · MARCH 2002

Impact Factor: 4.46 · DOI: 10.1021/la025563y

5 AUTHORS, INCLUDING:

Natalie Malikova
Pierre and Marie Curie University - Paris 6
51 PUBLICATIONS **980** CITATIONS
SEE PROFILE

Isabel Pastoriza-Santos
University of Vigo
146 PUBLICATIONS **8,847** CITATIONS
SEE PROFILE

Nicholas Kotov
University of Michigan
445 PUBLICATIONS **26,689** CITATIONS
SEE PROFILE

Layer-by-Layer Assembled Mixed Spherical and Planar Gold Nanoparticles: Control of Interparticle Interactions

Natalie Malikova,[†,‡] Isabel Pastoriza-Santos,[§] Martin Schierhorn,[§,||] Nicholas A. Kotov,*[,†] and Luis M. Liz-Marzán*[,§]

Department of Chemistry, Oklahoma State University, Stillwater, Oklahoma 74078, and Departamento de Química Física, Universidade de Vigo, 36200, Vigo, Spain

Received January 22, 2002. In Final Form: March 4, 2002

Gold nanoparticles (NPs) were prepared by reduction with salicylic acid in aqueous solution. The resulting dispersions were found to contain a mixture of flat triangular/hexagonal and smaller close-to-spherical NPs. As expected from theoretical considerations, such nanocolloids display two clearly differentiated surface plasmon bands at 540 and 860 nm associated with spherical and anisotropic triangular/hexagonal NPs, respectively. Layer-by-layer (LBL) assembly was used to deposit thin films of the Au colloids. UV−visible data indicate preferential adsorption of the flat particles on polyelectrolyte films. Importantly, a new band developed at 650 nm as the number of the Au NPs bilayers increased. This finding indicates that there exists a strong interaction between the NPs in adjacent layers, resulting in the surface plasmon absorption at a new wavelength. The insertion of extra polyelectrolyte or montmorillonite layers between the Au bilayers was shown to gradually reduce the interlayer interaction and resulted in the NP composite films with absorption spectra virtually identical to those of the original dispersion. The bilayer deposition sequence in LBL assembly, i.e. multilayer architecture, can be used to control the strength of NP−NP coupling in the layered composites.

Introduction

The optical properties of metal nanoparticles (NPs) have been intensively studied for the last few decades, because of strong catalytic properties, intense surface plasmon resonances, and strong surface enhanced and nonlinear optical properties. Surface plasmon effects arising from the coupling of conduction electrons with incident electromagnetic waves[1−3] are especially relevant in noble metals such as gold and silver, and the plasmon-related phenomena have been studied for them for a large number of scattering conditions at the NP interface.[4−6] Among them, the NP shape, dielectric environment, and interparticle distance are probably the most important parameters determining the surface plasmon frequency, since the oscillations of free electrons are largely dependent on the space available. While the oscillation path on metal spheres has very little variability, electrons in rods can oscillate both in a transversal and in a longitudinal mode,[4] which brings about two well-defined surface plasmon peaks. Similarly, metal spherical shells display two different plasmon bands, which depend on the thickness of the shell and the total diameter of the sphere.[5] The shape of flat silver NPs was recently found[7] to strongly affect the spectral position of the surface plasmon band.

Another fundamental parameter determining the surface plasmon resonance is the environment in which the metal NPs are embedded. For a dilute assembly of NPs in a dielectric, the refractive index of the dielectric is the most relevant factor, although any chemical moiety adsorbed onto the surface or present in its vicinity can also influence the surface plasmon resonance.[3] Dipole−dipole interactions play an important role in optics of metal NPs as well, and especially so for closely spaced NP films, as has been recently shown by Ung et al.[8] for assemblies on flat surfaces and by Caruso et al.[9] for assemblies on spheres. In these systems, the interparticle separation determines the plasmon oscillation frequency.

All these factors need to be taken into account tailoring the NP material to a particular application. For sensor devices, the dependence of the surface plasmon wavelength on the interparticle interactions can be the most significant parameter to consider. Thus, the search for the methods of control over the optical properties of noble metal NP materials is the subject of this work. The strength of NP−NP through-space coupling can be tuned by the variation of the spacing between the NP layers. This can be accomplished by the layer-by-layer assembly (LBL),[10,11] a new thin film preparation technique, which can be utilized for structural organization of a large variety of nanoparticles and nanocolloids.[12]

We present here the optical characterization of a mixture of isotropic and anisotropic gold NPs, both in dilute solution and assembled as thin films. Three principal findings of this work are the following: (1) Selection of a stabilizer (capping agent) affords the control of particle shapes. Well-

[†] Oklahoma State University.

[‡] On leave from Chemistry Department, Cambridge University, Cambridge, U.K.

[§] Universidade de Vigo.

[||] On leave from Department of Chemistry, Pennsylvania State University.

(1) Kreibig, U., Vollmer, M. *Optical Properties of Metal Clusters*; Springer: Berlin, 1995.
(2) Henglein, A. *J. Phys. Chem.* **1993**, *97*, 5457.
(3) Mulvaney, P. *Langmuir* **1996**, *12*, 788.
(4) van der Zande, B. M. I.; Böhmer, M. R.; Fokkink, L. G.; Schöneberger, C. *Langmuir* **2000**, *16*, 451.
(5) Oldenburg, S. J.; Averitt, R. D.; Westcott, S. L.; Halas N. J. *Chem. Phys. Lett.* **1998**, *288*, 243.
(6) Link, S.; El-Sayed, M. A. *J. Phys. Chem. B* **1999**, *103*, 8410.
(7) Jin, R.; Cao, Y. W.; Mirkin, C. A.; Kelly, K. L.; Schatz, G. C.; Zheng, J. G. *Science* **2001**, *294*, 1901.
(8) Ung, T.; Liz-Marzán, L. M.; Mulvaney, P. *J. Phys. Chem. B* **2001**, *105*, 3441.
(9) Caruso, F.; Spasova, M.; Salgueiriño-Maceira, V.; Liz-Marzán, L. M. *Adv. Mater.* **2001**, *13*, 1090.
(10) Mamedov, A. A.; Belov, A.; Giersig, M.; Mamedova, N. N.; Kotov, N. A. *J. Am. Chem. Soc.* **2001**, *123*, 7738.
(11) Pastoriza-Santos, I.; Koktysh, D. S.; Mamedov, A. A.; Giersig, M.; Kotov, N. A.; Liz-Marzán, L. M. *Langmuir* **2000**, *16*, 2731.
(12) Kotov, N. A., *MRS Bull.* **2001**, *26*, 992.

10.1021/la025563y CCC: $22.00
Published on Web 03/30/2002

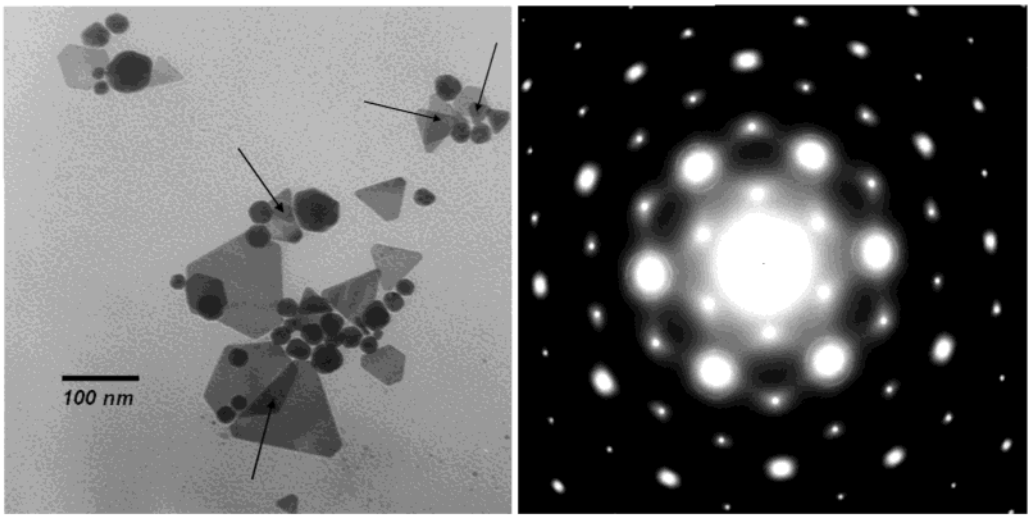

Figure 1. (a) Representative TEM image of gold NPs formed by reduction with salicylic acid. Both spheres and polygons are clearly visible. Arrows point to some places where two flat particles overlap. (b) Electron diffraction pattern from a single Au triangle with the electron beam perpendicular to the [111] plane. The spot array indicates a hexagonal structure.

defined NPs of triangular and related shapes were synthesized by a simple procedure. The synthesis of similarly shaped particles was recently reported for silver with comparable results.[7] Apart from occasional observations of gold triangles in small numbers,[13] this is the first synthetic recipe producing *spectroscopically legible* anisotropic, flat Au nanocolloids. (2) Flat NPs are deposited parallel to the substrate as evidenced by atomic force microscopy (AFM). This implies that the interparticle interactions between adjacent layers are strong, which can be seen by the appearance of a new absorption band. (3) The interaction between the layers can be controlled by depositing insulating layers of clay and/or polyelectrolytes between the gold nanoparticle layers.

Experimental Section

Tetrachloroauric acid trihydrate was obtained from Aldrich. Salicylic acid (≥99%) was purchased from Fluka. Poly(acrylic acid) (PAA), M_w 450000, and poly(diallyldimethylammonium chloride) (PDDA), M_w 400000−500000, were purchased from Aldrich. Montmorillonite clay was obtained from Alfa Aesar. Milli-Q deionized water (resistivity higher than 18 MΩ cm^{-1}) was used for all preparations.

Gold sols were prepared by reduction of chloroauric acid with salicylic acid, following the method reported by Okamoto and Hachisu,[15] though these authors reported a different particle morphology. After recrystallization of salicylic acid, 5 mL of a saturated solution was added to 100 mL of 0.05 wt % chloroauric acid neutralized by NaOH, followed by heating at 80 °C for 10 min.

Layer by layer assembly was performed by sequential dipping of a glass slide in aqueous solutions of positively charged polyelectrolyte and negatively charged polyelectrolyte or nanoparticle dispersion following the general procedure outlined in previous publications.[9,11,12] The optimal pH for adsorption was chosen by monitoring through UV−visible spectroscopy. Separator layers of PDDA and PAA were deposited from solutions of 0.1 wt % and pH 7.0.

AFM images were taken by using a Nanoscope IIIa instrument operating in the tapping mode with standard silicon nitride tips. Typically, the surface was scanned at 2 Hz with 256 lines per image resolution and 1.2−4.0 V setpoint.

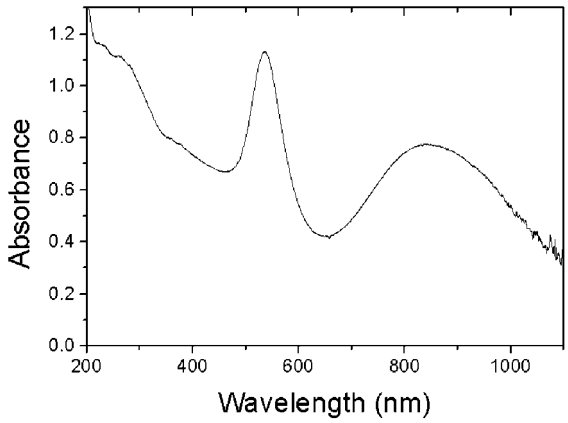

Figure 2. UV−visible spectrum measured from a dilute sol containing the particles shown in Figure 1.

Transmission electron microscopy (TEM) was measured with a JEOL JEM 1010 at an acceleration voltage of 100 kV.

UV−visible spectroscopy was measured with a Hewlett-Packard HP 8453 A diode-array spectrophotometer. The glass slides bearing the multilayer films were placed perpendicular to the beam. The spectra presented were averaged on the basis of typically three spectral scans. During the successive depositions, UV−visible spectra were taken from the same area of the sample.

Results and Discussion

Gold Nanoparticle Formation. The NPs obtained were characterized by TEM and UV−visible spectroscopy. A representative TEM image is shown in Figure 1. Gold NPs with several different shapes are formed, including large polygons (mainly triangles and hexagons) as well as smaller, polydisperse spheres. The lower contrast observed for the polygons suggests that they are flat, unlike the spherical NPs around them. Also, at some places (see arrows) two planar particles overlap, yielding a darker region. The electron diffraction analysis confirmed the hexagonal structure of a single triangle lying flat on the TEM grid. Such a flat geometry imposes strong restrictions for the oscillation frequency of the free conduction electrons, which is directly reflected on the optical properties of the dispersion.

The UV−visible spectrum shown in Figure 2 was measured from the gold dispersion in water. The spectrum shows two distinct plasmon absorption bands centered at

(13) Turkevich, J.; Stevenson, P. C.; Hillier, J. *Discuss. Faraday Soc.* **1954**, *11*, 55.
(14) Mamedov, A.; Ostrander, J. W.; Aliev, F.; Kotov, N. A., *Langmuir* **2000**, *16*, 3941.
(15) Okamoto, S.; Hachisu, S. *J. Colloid Interface Sci.* **1977**, *62*, 172.

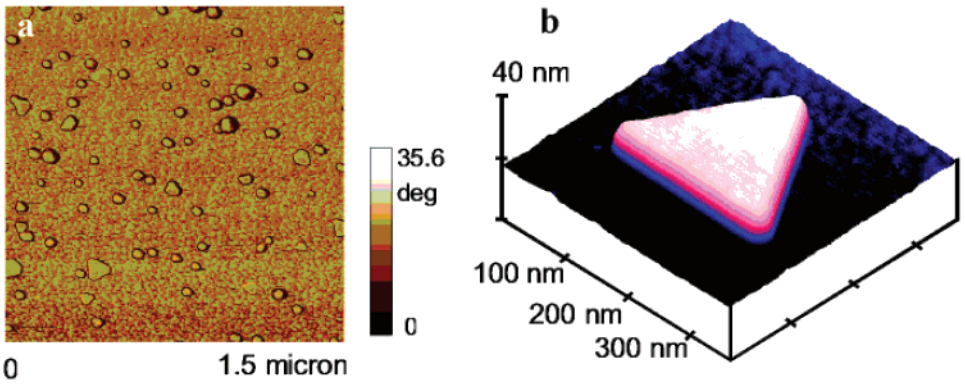

Figure 3. Atomic force microscopy of a PDDA/Au bilayer deposited on a Si wafer: (a) large area phase contrast image; (b) closer topographic view of a triangular particle.

540 and 860 nm. The band at higher energy is located at typical values for Au spheres, with a certain distortion with respect to the spherical shape. However, the band at 860 nm could only correspond to a resonance over much larger distances (observed for the longitudinal resonance in nanorods or for nanoshells) or to tight aggregates formed by smaller NPs. The last possibility is discarded because of the long-term stability of the colloid and because only separate NPs were found under TEM observation. The band is broad because of the relatively high polydispersity, both in size and shape, which implies quite a broad range of possible resonance frequencies. Therefore, the 860 nm band is attributed to the surface plasmon band in flat gold particles of triangular and related shapes seen in Figure 1. The anisotropic morphology and specific shape of the particles make possible the plasmon transition over the long distances. Although three well-differentiated bands are expected for these systems,[7] because of the relatively low concentration of polygons, the absorption by the spheres screens the out-of-plane quadrupole resonance (located at lower wavelengths).

Layer-by-Layer Assembly. The procedure used for the assembly of the gold NPs is based on the layer-by-layer approach,[16,17] i.e., the use of oppositely charged species for an alternate deposition onto a flat substrate. The control of NP−NP coupling with this technique was previously attempted for magnetic NPs by LBL;[14,18] however little change in magnetic characteristics has been observed. The electron interactions between the gold NPs are of much shorter range than magnetic dipole interactions and result in a strong shift in the frequency of the surface plasmon resonance. The later can be easily observed by UV−visible absorption spectroscopy, which can be utilized to monitor the strength of the particle interactions in adjacent layers.

The gold NPs are negatively charged owing to the stabilizing layer of salicylic acid, and therefore, a positively charged polyelectrolyte was chosen as an LBL partner macromolecule for them. The morphology of the deposited monolayers was studied by AFM. A typical image is shown in Figure 3a, where it can be observed that the proportion of polygons is relatively low, as compared to spheres, which form a compact monolayer on the background. It is also interesting to note that AFM measurements confirm the TEM observation that the triangular and hexagonal particles are flat (Figure 3b), with lateral dimensions much larger than their height. It can also be clearly seen that

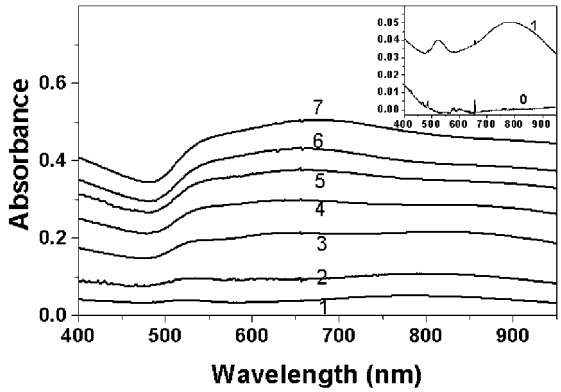

Figure 4. UV−vis spectra of successive LBL assembled (PDDA/Au)$_n$ bilayers (the number of the deposition cycles n is given as the trace number). The inset shows the background absorption of the substrate and the first (PDDA/Au)$_1$ bilayer.

the flat particles are deposited parallel to the substrate similarly to montmorillonite sheets studied previously.[19]

The high density of adsorbed NPs translated at the macroscale into a high optical uniformity of the coatings over the entire area of the samples prepared. UV−visible absorption spectra acquired for sequentially deposited PDDA/Au bilayers, i.e., for coatings (PDDA/Au)$_n$ where n is the number of the deposition cycles, show that the absorbance gradually increases with every new bilayer (Figure 4). It can also be seen in the inset that the first (PDDA/Au) bilayer displays absorption bands at 525 and 790 nm, which are very similar to those of the starting NP dispersion. The slight shift of both peaks can be related to the change in environment after the deposition, since at least one side is surrounded by air. Interestingly, the intensity of the absorption band for triangular NPs significantly increases with respect to the band for spherical NPs (Figure 4 insert vs Figure 2). This can be rationalized as the result of stronger PDDA-NP attraction forces involving anisotropic flat triangular NPs than those with spherical ones resulting in the preferential adsorption of the flat NPs. In the assessment of the absorption preference, the UV−visible data are more representative than AFM images because they provide cumulative information about a large area of the sample. Additionally, smaller spherical NPs can be easily adsorbed on top of the triangles,[20] thereby masking them both in topography and phase scans.

(16) Decher, G. *Science* **1997**, *277*, 1232.
(17) Kotov, N. A.; Dekàny, I.; Fendler, J. H. *J. Phys. Chem.* **1995**, *99*, 13065.
(18) Aliev, F.; Correa-Duarte, M. A.; Mamedov, A.; Ostrander, J. W.; Giersig, M. Liz-Marzán, L. M.; Kotov, N. A., *Adv. Mater.* **1999,** *11*, 1006.
(19) Kotov N. A.; Magonov S., Tropsha E., *Chem. Mater.* **1998**, *9*, 886.
(20) Rogach, A.; Koktysh, D.; Harrison, M.; Kotov, N. A., *Chem. Mater.* **2000**, *12*, 1526.

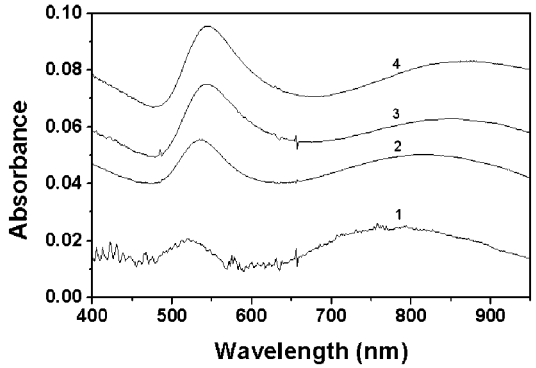

Figure 5. UV−vis spectra of sequentially deposited (PDDA/Au/PDDA/PAA)$_n$, $n = 1-4$.

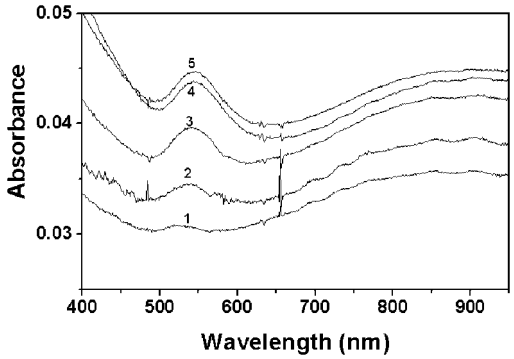

Figure 6. UV−vis absorption spectra of (PDDA/Au/PDDA/clay)$_n$, $n = 1-5$ film deposition cycles.

Importantly, a new optical feature develops as the number of layers increases. An intense band is formed between the two previous ones becoming clearly visible in the fourth layer and becoming dominant by the seventh bilayer (Figure 4). This new band at 650 nm is attributed to the interparticle interactions between neighboring monolayers, which can be supported by the extensive literature on the dependence of surface plasmon band on interparticle separation.[8,21]

Since the NP−NP coupling typically results in the red shift of the surface plasmon bands, we believe that the parent transition for the new band is that in the spherical NPs at 525 nm. In the multilayer assembly, they interact both with similar spherical NPs and triangular ones. In the latter case, the coupling strength should be higher than in the former because of the geometry of sphere on a plane results in greater integral electrostatic attraction than that between two spheres. The variety of different geometrical arrangements causes band broadening, which can be seen in Figure 4. Note that the transversal modes of the flat NPs can also contribute to this new band. At the same time, the longitudinal modes of flat NPs should also be red-shifted and show up in the range of 800−900 nm partially overlapping with the new band at 650 nm.

To confirm the origin of this new band, further LBL experiments were performed by taking advantage of the structural control afforded by the LBL technique and different insulting layers, which can be used to separate the Au NPs bilayers. This was accomplished by depositing a polyelectrolyte (PDDA/PAA) bilayer between PDDA/Au strata as a nanoscale spacer (Figure 5). It is clear that by placing an additional polymeric region between the NP bilayers reduces the interactions of the adjacent Au NPs layers and the band at 650 nm does not develop. However, there is a noticeable red shift of both plasmon bands as the number of layers increases, showing that there is still a certain electronic communication between neighboring layers.

Therefore, further experiments were carried out to obtain virtually electronically independent surface plasmon oscillations in each Au NPs layer. To achieve that, the separation layers were made from montmorillonite clay platelets that are (1) better electrical insulators than polyelectrolytes and (2) reduce interdigitation of the adjacent layers due to their sheetlike morphology.[10,12,14,19] Thus, the layered stacks with a repeat unit of (PDDA/Au/PDDA/clay)$_n$ were made and their optical spectra are shown in Figure 6. As expected, the improved insulation and better separation of the adjacent gold NPs bilayers lead to a constant position of both plasmon absorption bands in every deposition cycle. It should be noted that there is still a slight red shift of the maxima in comparison to the UV−visible spectrum of the dispersion because of the refractive index increase after the deposition of the montmorillonite sheets.

Conclusions

In this paper we have shown that anisotropic gold NPs can be easily synthesized by selecting an appropriate stabilizer, salicylic acid, albeit in a mixture with nearly spherical particles. The UV−visible spectra of aqueous dispersions of such NPs contain two distinct absorption bands, assigned to the plasmon resonance within smaller, spherical particles, and to a longitudinal mode within larger, flat NPs. The shape of the spectrum is maintained when a monolayer of NPs is deposited on a flat substrate using the layer-by-layer approach. Deposition of multiple layers leads to the formation of a new band at 650 nm due to NP−NP coupling in the adjacent bilayers, as demonstrated through the deposition of inert intermediate, polymeric, or inorganic layers leading to the suppression of the new band. Importantly, the sequence of the deposited LBL layers can be utilized for the gradual control of interparticle interactions, when the thickness of the layers is comparable with the characteristic length of the interactions. The demonstrated structural control over the optical properties of the NP assemblies can be applied for the design of thin film sensors with a transduction mechanism based on the variations of spacing between the Au layers.

Acknowledgment. L.M.L.-M. acknowledges financial support from the Spanish Xunta de Galicia, (Project No. PGIDT01PXI30106PR) and Ministerio de Ciencia y Tecnología (Project No. BQU2001-3799). I.P.-S. acknowledges the Spanish Ministerio de Educación y Cultura for a personal grant. N.A.K. thanks NSF CAREER (CHE-9876265), NSF Biophotonics Initiative (BES-0119483), AFOSR (F49620-99-C-0072), and OCAST (AR99(2)-026) for the financial support of this research. The authors are indebted to J. Méndez from the CACTI of Vigo University for his assistance with TEM measurements and to Dmitry S. Koktysh from Oklahoma State University for his help with the AFM imaging. N.M. and N.A.K. acknowledge the travel support for N.M. from Cambridge University, U.K.

LA025563Y

(21) Schmitt, J.; Mächtle, P.; Eck, D.; Möhwald, H.; Helm, C. A. *Langmuir* **1999**, *15*, 3256.